

# A Hybrid Silicon Sampled Grating DBR Tunable Laser

Matthew N. Sysak<sup>1</sup>, Joel O. Anthes<sup>2</sup>, Di Liang<sup>2</sup>, John E. Bowers<sup>2</sup>, Omri Raday<sup>3</sup>,  
Richard Jones<sup>1</sup>

<sup>1</sup>Intel Corporation, 2200 Mission College Blvd. SC12-236 Santa Clara, Ca 95054, USA

<sup>2</sup>Department of Electrical Engineering, University of California, Santa Barbara, CA 93106, USA

<sup>3</sup>Numonyx Corporation, Qiryat Gat, 82109, Israel

Phone: 805-893-5828, Fax: 805-893-7990, Email: matthew.n.sysak@intel.com

## Abstract

We present a hybrid silicon sampled grating DBR laser fabricated using quantum well intermixing. The laser utilizes two III-V bandgaps spanning >80 nm. Output power is >2.5mW with CW lasing to 40°C and tuning >12nm.

## I. Introduction

There has been a large body of research focused on the development of an optical source that is compatible with silicon photonics and CMOS fabrication. One of the more promising technologies in this area consists of wafer bonding a III-V quantum well active region to a silicon on insulator (SOI) wafer with pre-fabricated optical waveguides. In this approach, the III-V material is used for optical gain and the silicon is used for passive optical routing. Several types of devices have been demonstrated using this wafer bonding technique including ring lasers, photodetectors, modulators, and distributed feedback (DFB) lasers [1, 2, 3]. However, one of the major drawbacks to this approach is that only devices with a single III-V material bandgap can be realized without complex epitaxial structures or additional bonding. Integrated photonic circuits that benefit from multiple bandedges, such as tunable lasers and tunable lasers integrated with electroabsorption modulators, have not been demonstrated.

In this work we present a hybrid silicon sampled grating distributed Bragg reflector (SGDBR) tunable laser that utilizes multiple III-V material bandgaps. The device is fabricated using quantum well intermixing (QWI) where disordering of the quantum well active region is performed before bonding to shift the bandgap of the as-grown III-V material. The SGDBR laser utilizes two material bandgaps that have photoluminescence peaks at 1520 nm for optical gain and 1440 nm for mirrors, phase, and taper regions. Output power from the laser is >2.5 mW, CW lasing up to 40 °C is achieved, and current injection into the III-V mirror regions provides tuning over >13 nm.

## II. Device Overview

A scanning electron-micrograph (SEM) image of an array of four hybrid silicon SGDBR lasers is shown in Fig. 1. Each device includes a 600 μm backside absorber, 650 μm rear mirror, 80 μm phase region, 550 μm gain region, 270 μm long front mirror, and a 100 μm long taper,. The laser array is diced at a 7 degree angle, polished, and AR coated to reduce back reflections into the laser cavity from the silicon waveguide/air interface. Taper regions identical to that used for amplifiers in [5] are used to transition the optical mode from the hybrid waveguide to an SOI waveguide.

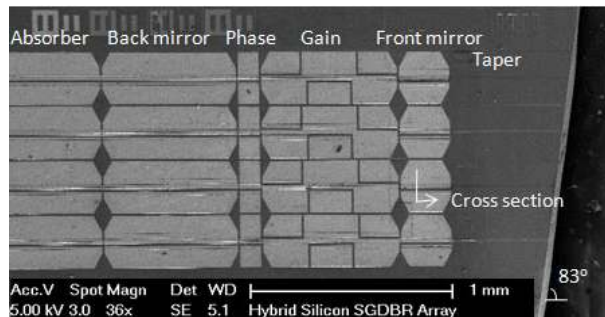


Fig 1. SEM of an array of four hybrid silicon sampled grating DBR lasers. The air/inP chip interface is diced, polished, and AR coated to reduce back reflections into the laser cavity.

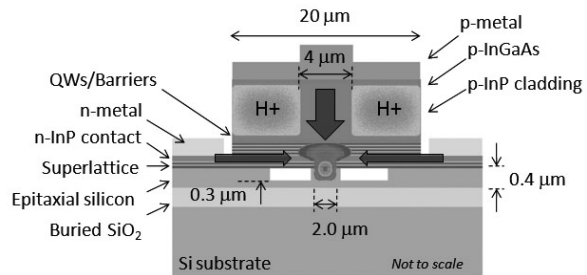


Fig 2. Cross section of hybrid silicon SGDBR laser in gain, phase, backside absorber and mirror regions. Current is injected from the n and p contacts into the quantum wells for optical gain.

Fig. 2 shows a cross section of the gain, passive, and backside absorber regions. All laser sections employ a 20  $\mu\text{m}$  wide mesa, silicon epitaxial height of 0.4  $\mu\text{m}$ , a rib etch depth of 0.3  $\mu\text{m}$ , and a silicon waveguide width of 2  $\mu\text{m}$ . A 4  $\mu\text{m}$  wide proton ( $\text{H}^+$ ) implant channel is used for current confinement. The rear mirror has fourteen 7.6  $\mu\text{m}$  wide grating bursts and a 46.4  $\mu\text{m}$  sampling period and the front mirror has five 5.2  $\mu\text{m}$  wide grating bursts with a 52.4  $\mu\text{m}$  sampling period. The grating etch depth into the III-V is 100 nm, resulting in an experimentally measured  $\kappa$  of 165  $\text{cm}^{-1}$ . A 10  $\mu\text{m}$  wide proton implant is used to electrically isolate the gain, phase, mirror, and taper regions. The resistance between laser sections is  $>10 \text{ k}\Omega$ .

### III. Device fabrication and Quantum Well Intermixing

Fabrication of the sampled grating DBR lasers is divided into pre-bonding, bonding, and post-bonding steps. Prebonding includes QWI, patterning and etching first order gratings into the III-V material, and patterning shallow etched waveguides into the SOI. Following prebonding, the SOI and III-V wafers are bonded together using a low temperature plasma assisted bonding process [1]. After bonding, fabrication is identical to that in [1], and includes patterning and etching III-V mesas, depositing n and p metal contacts, proton implantation, and probe metallization.

The QWI process is based on implant enhanced intermixing technology [6]. In this process, vacancies are generated using ion implantation into a sacrificial InP buffer layer, then diffused through the quantum well active region where they cause disordering between quantum wells and barriers. The disordering modifies the active region concentration profile and hence the potential profile, and shifts the emission wavelength from the wells and barriers. Details of the as-grown III-V structure used for the hybrid silicon SGDBR lasers along with details of the quantum well intermixing process are outlined in Fig. 3(a) – 3(c). The process begins with a blanket phosphorous implant into the sacrificial InP layer. III-V regions that will be used for optical gain are masked from the implant using a  $\text{SiN}_x$  layer deposited using PECVD. The implanted sample is then subjected to a rapid thermal anneal at 725  $^\circ\text{C}$  to cause the atomic interdiffusion. For the regions that were protected from the implant (optical gain regions) the lack of vacancies in the buffer layer prevents intermixing. After rapid thermal annealing the InP buffer is removed to planarize the surface before bonding. The Photoluminescence peak shift as a function of RTA time is shown in Fig 4 for both implant protected and implanted III-V regions. Initially, the large atomic concentration gradient between the QWs and barriers cause rapid atomic interdiffusion, and hence a rapid photoluminescence shift. However, as annealing continues and the concentration gradient at the QW/barrier interface decreases, the rate of PL shift is reduced until it finally saturates. In the hybrid silicon III-V base structure, the PL shift as a function of RTA time saturates with 330s of annealing and a 90 nm separation between the implanted (mirrors, phase, and taper regions) and implant protected (gain) regions. To minimize the optical loss associated with the Urbach tail of the passive region material bandgap, an anneal time of 330s is used in the QWI process to achieve the largest possible separation between the PL of the gain and the mirrors, phase, and tapers.

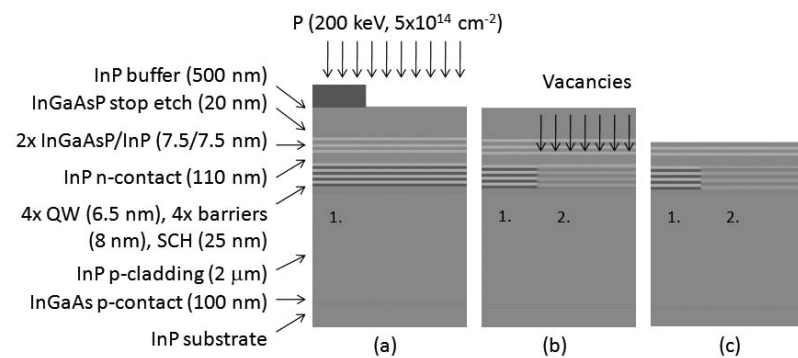


Fig 3. Overview of quantum well intermixing process. Discrete bandgaps generated are labeled 1 and 2. (a) Details of initial III-hybrid laser base structure and implantation of phosphorous into the sacrificial InP buffer. (b) Diffusion of vacancies from InP buffer through QW active region to generate bandgap 2. (c) Removal of InP buffer layer to planarize the III-V before bonding.

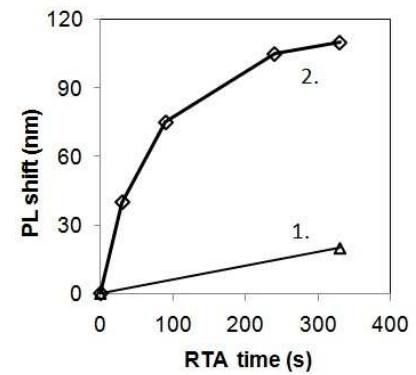


Fig. 4. Photoluminescence peak shift as a function of RTA time. The saturation of the PL shift is due to the reduction in concentration gradient between QWs and barriers as RTA continues.

### III. Sampled Grating DBR Laser performance

Continuous wave output power-gain section bias current-gain section voltage (LIV) results are shown in Fig. 5 for a laser with a 2.0  $\mu\text{m}$  wide silicon waveguide. CW lasing is achieved up to 40  $^\circ\text{C}$  with output power  $>2.5 \text{ mW}$  and a

40 mA threshold at 10 °C. The series resistance of the gain section is 15 Ω. Dips in the LI characteristics are a result of cavity modes moving through the mirror reflectivity envelope as heating in the SGDBR gain region changes the cavity effective index [7]. Fiber coupled output spectra from the SGDBR laser with a gain bias of 140 mA, a fixed backside temperature of 25 °C, and three different current injection levels into both front and rear mirrors are shown in Fig 6. With no current injection into the mirrors, the SGDBR lasing wavelength is 1506.5 nm. However, with 20 mA bias current into the front mirror and 0 mA bias in the rear mirror, the SGDBR output is shifted by one supermode to an operating wavelength of 1501 nm. Similarly, with 10 mA bias current into the rear mirror and 0 mA bias into the front mirror, the laser is shifted by one supermode to a lasing wavelength of 1514 nm. For each of the operating wavelengths, the side mode suppression ratio (SMSR) is greater is >30 dB. The increased amplified spontaneous emission at lower wavelengths is a result of band-filling, which reduces optical loss in the SGDBR front mirror. The limited tuning range when current is injected into the mirrors is a result of several factors, including high laser thermal impedance [8] and a small laser active region volume (four QWs).

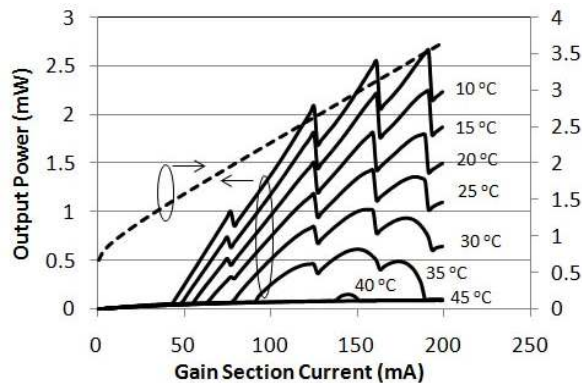


Fig. 5. LIV characteristics from hybrid silicon SGDBR laser. Output power is > 2.5 mW at 10 °C with 40 mA threshold. Series resistance is 15 Ω.

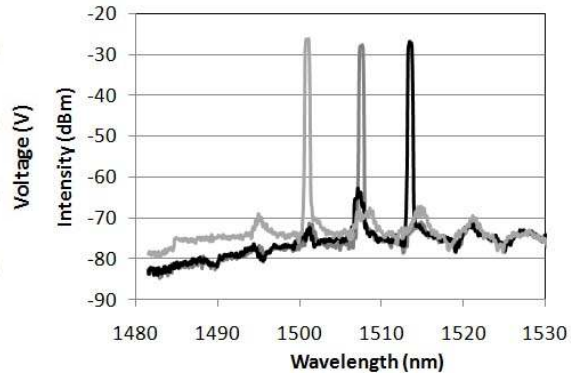


Fig. 6. Fiber coupled SGDBR spectra with 140 mA gain bias at 25 °C. With no front or rear mirror bias the lasing wavelength is 1506.5 nm. With 20 mA bias in the back mirror and 0 mA in the front mirror, the lasing wavelength is 1501 nm. With 0 mA in the rear mirror and 10 mA bias in the front mirror, the lasing wavelength is 1514 nm.

#### IV. Conclusions

We have demonstrated a hybrid silicon sampled grating DBR tunable laser. The device uses multiple III-V material bandgaps for mirrors and optical gain regions separated by >80 nm that are generated using a quantum well intermixing process. The SGDBR lasers have an output power >2.5 mW at 10 °C with a threshold of 40 mA and tuning over 13 nm. This work represents the first implementation of multiple III-V material bandgaps on the hybrid silicon evanescent device platform.

#### V. References

- [1] A. W. Fang, R. Jones, H. Park, O. Cohen, O. Raday, M. J. Paniccia, and J. E. Bowers, "Integrated AlGaInAs-silicon evanescent race track laser and photodetector," *Optics Express* **5**, 2315-2322, (2007).
- [2] Y.-H. Kuo, H.-W. Chen, and J. E. Bowers, "A hybrid silicon evanescent electroabsorption modulator," *OFC 2008*, San Diego, CA, (2008).
- [3] A. W. Fang, E. Lively, Y.-H. Kuo, D. Liang, and J. E. Bowers, "Distributed Feedback Silicon Evanescent Laser," *OFC/NFOEC*, postdeadline session PDP15, 2008.
- [4] V. Jayaraman, Z. Chuang, and L. A. Coldren, "Theory, Design, and Performance of Extended Tuning Range Semiconductor Lasers with Sampled Gratings," *IEEE Journal of Quantum Electronics*, **29**, (6), (1993).
- [5] H. Park, Y.-H. Kuo, A. W. Fang, R. Jones, O. Cohen, M. J. Paniccia, and J. E. Bowers, "A hybrid AlGaInAs-silicon evanescent preamplifier and photodetector," *Optics Express*, **15**, (2007).
- [6] E.J. Skogen, J.S. Barton, S.P. Denbaars, and L.A. Coldren, "A Quantum-Well-Intermixing Process for Wavelength-Agile Photonic Integrated Circuits," *Journal of Selected Topics in Quantum Electronics*, **8**, 863-869, (2002)
- [7] Jen Buus book H. Park, Y.-H. Kuo, A. W. Fang, R. Jones, O. Cohen, M. J. Paniccia, and J. E. Bowers, "A hybrid AlGaInAs-silicon evanescent preamplifier and photodetector," *Optics Express*, **15**, (2007).
- [8] M. N. Sysak, H. Park, A. W. Fang, J. E. Bowers, R. Jones, O. Cohen, O. Raday, and M. Paniccia, "Experimental and theoretical thermal analysis of a Hybrid Silicon Evanescent Laser," *Optics Express*, **15**, 15041-15046, (2007).